

Mucoadhesive chitosan-coated nanostructured lipid carriers for oral delivery of amphotericin B

Janet Tan Sui Ling¹, Nashiru Billa^{1*}, Clive J. Roberts²

Janet Tan Sui Ling: khyx5jts@exmail.nottingham.edu.my

¹ School of Pharmacy, University of Nottingham, Malaysia Campus
43500 Semenyih, Selangor
Malaysia

Clive J Roberts: clive.roberts@nottingham.ac.uk

² School of Pharmacy, University of Nottingham
University Park
Nottingham
NG7 2RD
UK
ORCID ID: 0000-0001-9443-3445

*Corresponding author (Nashiru.Billa@nottingham.edu.my)

Tel: +60389248211

ORCID ID: 0000-0002-8496-1882

Abstract

This study describes the properties of an amphotericin B-containing mucoadhesive nanostructured lipid carrier (NLC), with the intent to maximize uptake within the gastrointestinal tract. We have reported previously that lipid nanoparticles can significantly improve the oral bioavailability of amphotericin B (AmpB). On the other hand, the aggregation state of AmpB within the NLC has been ascribed to some of the side effects resulting from IV administration. In the undissolved state, AmpB (UAmpB) exhibited the safer monomeric conformation in contrast to AmpB in the dissolved state (DAmpB), which was aggregated. Chitosan-coated NLC (ChiAmpB NLC) presented a slightly slower AmpB release profile as compared to the uncoated formulation, achieving 26.1 % release in 5 hours. Furthermore, the ChiAmpB NLC formulation appeared to prevent the expulsion of AmpB upon exposure to simulated gastrointestinal pH media, whereby up to 63.9 % of AmpB was retained in the NLC compared to 56.1 % in the uncoated formulation. The

ChiAmpB NLC demonstrated mucoadhesive properties in pH 5.8 and 6.8. Thus, the ChiAmpB NLC formulation is well-primed for pharmacokinetic studies to investigate whether delayed gastrointestinal transit may be exploited to improve the systemic bioavailability of AmpB, whilst simultaneously addressing the side-effect concerns of AmpB.

Keywords: amphotericin B, nanostructured lipid carriers, oral, mucoadhesion, aggregation states

1. Introduction

Amphotericin B (AmpB) is a broad spectrum antifungal agent commonly used to treat invasive systemic fungal infections and visceral leishmaniasis (Legrand et al. 1992). It has a large glycosylated lactone ring, coupled with asymmetrical distribution of hydrophobic polyene chromophore and hydrophilic polyhydroxyl groups (Jung et al. 2009; Silva et al. 2013). Due to its amphipathic nature, AmpB tends to self-aggregate in aqueous solutions, forming, dimers or polyaggregates. The dimers are usually associated with the most toxic properties of AmpB and unfortunately this is the predominant state in the reconstituted marketed intravenous (IV) formulation, Fungizone® (Barwicz et al. 1992; Raquel Espada et al. 2008). AmpB exerts its antifungal properties by binding to ergosterol within fungal membranes, forming transmembrane pores that allow depletion of intracellular ions, which eventually lead to the cell death. In a similar fashion, AmpB also binds to mammalian cholesterol within the plasma membrane, which lead to severe side effects, notably nephrotoxicity (Butani et al. 2016). This is the hallmark of the toxic effects of the dimers mentioned above (Radwan et al. 2017). There is evidence that when delivered orally, these side-effects are minimized primarily due to the omission of the excipients used in the IV formula and crucially because of an impeded rate and extent of absorption of raw AmpB from the gastrointestinal tract (Kayser et al. 2003; Radwan et al. 2017; Liu et al. 2017). The oral bioavailability of AmpB can be boosted through formulation intervention as we have recently shown using solid lipid nanoparticles (SLNs) (Hilda Amekyeh et al. 2015). However, it was the extent of absorption that is improved rather than the rate of absorption, which suggests a possible lymphatic uptake pathway for the SLN. On the other hand, nanostructured

lipid carriers (NLC) comprise of an admixture of solid lipids and liquid oils which distort the solid lipid matrix hence arrests crystal growth and drug expulsion during storage as the case is with SLNs (Muchow et al. 2008). In addition, the NLC protect against possible enzymatic degradation and can accommodate relatively higher levels of cargoes than the SLNs (Yoon et al. 2013; Yostawonkul et al. 2017; Liu et al. 2017).

Several investigations on the oral delivery of AmpB have been conducted which employ a wide range of carrier systems. Some of these include polymeric nanoparticle carbon nanotubes, nanosuspensions, polymer lipid hybrid nanoparticles, solid lipid nanoparticles (SLN), cubosomes, emulsions and cochleates (Santangelo et al. 2000; Nahar et al. 2008; Italia et al. 2009; Wasan et al. 2009; Benincasa et al. 2011; Jain et al. 2012; Van De Ven et al. 2012; Yang et al. 2012; Tan & Billa 2014; H. Amekyeh et al. 2015; Chaudhari et al. 2016; Hussain et al. 2016; Amekyeh et al. 2017).

In terms of novelty on the current work and in advancement of the oral AmpB SLN formulation developed in our labs (Amekyeh et al. 2015), we have sought to exploit a sluggish transit of the NLC within the gastrointestinal tract in order to maximize uptake via the lymphatic pathway by way of coating the NLC with chitosan. Chitosan, a natural, non-toxic, biocompatible polycationic polysaccharide, derived from partial deacetylation of chitin was employed as the mucoadhesive polymer coating (Sandri et al. 2017). Therefore, this piece of work reports on the formulation and characterisation of uncoated and chitosan-coated AmpB-loaded NLC. We hypothesise that through mucoadhesion of the NLC we will confer a prolonged gastrointestinal transit in the small intestine which would result in improved uptake via lymph and hence improve bioavailability of AmpB. Furthermore, we are cognizant of the correlation between the aggregated state of AmpB and its toxicity. We exploited the pH-solubility and stability profiles of AmpB under alkaline conditions during the formulation of the NLC, which assumes the monomeric configuration. This configuration is known to manifest fewer side effects (Lance et al. 1995; Gagoś et al. 2008; Santos et al. 2012; Caldeira et al. 2015).

2. Materials and method

2.1. Materials

Beeswax and coconut oil were purchased from Acros Organics, New Jersey, USA. Chitosan (low molecular weight), porcine gastric mucin (type III), phosphate buffered saline tablets (PBS) and potassium phosphate monobasic were purchased from Sigma Aldrich Co. LLC., Missouri, USA; amphotericin B from Fisher Scientific, India. Soya lecithin was purchased from MP Biomedicals (Illkirch, France) and acetic acid was obtained from R&M Chemicals, India. All reagents and solvents used of analytical and HPLC grades respectively. Deionised water used was 18.2 MΩ.cm at 25 °C filtered through a Milli-Q filter, (Millipore Corp., Bedford, USA).

2.2. Formulation of AmpB-loaded NLC (AmpB NLC)

AmpB was incorporated during the formulation of the NLC either in a dissolved state (DAmpB) or undissolved state (UAmpB), at the initial step of preparation (method 1) or at the final step in the NLC formulation (method 2). DAmpB comprised of 10 mg/mL of AmpB in 0.1 M NaOH.

Method 1: Briefly, the oily phase (OP), comprised of 290 mg of beeswax and 10 mg of coconut oil was melted at 70 °C. AmpB either in undissolved or dissolved state was added to the melted lipids and mixed. The aqueous phase (AP), consisted of 50 mg of lecithin, 50 mg of Tween - 80 and 10 mL of deionised water was stirred at 500 rpm using a magnetic stirrer for 45 minutes at 70 °C and then added to the melted OP above. The resulting mixture was homogenised at 12,400 rpm for 8 minutes using a high speed homogeniser (Ultra-Turrax T25, Germany). The coarse emulsion was further subjected to probe ultrasonication (Q500 QSonica, Newtown, CT, USA) at 20 % amplitude for 8 minutes. Finally, the emulsion was added into sufficient deionised water (4 °C) under stirring to a total of 100 mL.

Method 2: The preparation of AmpB NLC formulation was similar to method 1 except that the incorporation of AmpB occurred at the final step of the formulation, in which the AmpB was added to the deionised water (4 °C) after ultrasonication of the emulsion (Santos et al. 2012; Caldeira et al. 2015). The incorporation of UAmpB was not feasible under this method due to precipitation thus, only DAmpB was utilised.

2.3. Formulation of chitosan-coated AmpB-loaded NLC (ChiAmpB NLC)

The physical adsorption of chitosan on the formulated NLC was done by addition of 0.2 %w/v chitosan solution in 1 % acetic acid dropwise into the NLC formulations at a ratio of 1:40 v/v under mechanical stirring at 250 rpm for 15 minutes at room temperature.

2.4. Physical properties of the formulations

2.4.1. Particle size, polydispersity index (PDI) and zeta potential

The particle size, polydispersity index (PDI) and zeta potential (ζ) of the AmpB NLC and ChiAmpB NLC formulations were measured using Zetasizer Nano ZS (Malvern, UK). Prior analysis, the samples were diluted appropriately using deionised water to avoid multiple scattering. All measurements were carried out in triplicate at 25 °C and results were expressed as mean \pm standard deviation.

2.4.2. Aggregation states of AmpB NLC and ChiAmpB NLC formulations

The predominant aggregation state of AmpB in the different formulations was characterised using a UV-visible spectrometer (Epoch Microplate Spectrophotometer, Bio Tek Instruments, USA). Absorption spectra from the formulations were recorded from 300-450 nm with a resolution of 1 nm at room temperature. All formulations were diluted with deionised water (1:10 v/v) so that results were within the linear sensitivity of the instrument. The absorbance from the blank formulations was also measured in order to eliminate effects due to artifacts. The predominant aggregation state of AmpB within each spectrum was determined by calculating the ratio of absorbance at 332 nm (peak of the dimer) to that at 407 nm (peak of the monomer).

2.4.3. Morphology and topography

The morphology and topography of the formulations were examined using a scanning transmission electron microscopy (STEM) system, Quanta 400F (FEI Company, USA). Prior to analysis, the undiluted samples were applied on a formvar-coated copper grids without fixation and air-dried. Samples were observed under scanning transmission of 20 kV in high vacuum.

2.4.4. Encapsulation efficiency (% EE) and drug loading (% DL)

A direct method was used to determine the encapsulation efficiency (% EE) and drug loading (% DL) in AmpB NLC and ChiAmpB NLC formulations. Briefly, 1 mL of the formulation was precipitated by addition of 10 mL of acetonitrile. The resulting mixture was centrifuged at 20 000 rpm for 10 minutes at 4 °C. The supernatant was decanted and DMSO: MeOH (1:1) was added to the pellet containing the encapsulated drug which was heated at 70 °C. The amount of AmpB was measured using high performance liquid chromatography (HPLC) system (1260 Series, from Agilent technologies, Waldbronn, Germany, equipped with a 15 cm x 4.6 mm reversed-phase C-18 column, Hypersil Gold, ThermoFisher Scientific, Waltham, United States, 5 µm particle size stationary phase). A mixture of 60 % 2.5 mM EDTA and 40 % acetonitrile was used as the mobile phase at a flow rate of 1.2 mL/min, with the wavelength set at 408 nm. Results are expressed as mean ± standard deviation. The linear regression of the calibration curve was obtained for AmpB at a concentration of 0.1-100.0 µg/mL in DMSO: MeOH (408 nm) with r^2 of 0.9998. The % EE and % DL were calculated using the following equations:

$$\%EE = \frac{W_s}{W_t} 100 \dots\dots\dots (1)$$

$$\%DL = \frac{W_s}{W_N} 100 \dots\dots\dots (2)$$

where, W_T is the amount of AmpB in the system, W_S is the amount of AmpB detected in the sediment and W_N weight of nanoparticles obtained from freeze-dried sediments.

2.5. In vitro release studies

A 50 µl aliquot of AmpB NLC or ChiAmpB NLC formulations was mixed with 950 µl phosphate buffered saline (pH 7.4) containing 1 % Tween - 80 into six seeded tubes and rotated at 120 rpm in a rotary shaker (WiseCube®, Witeg Inc., Germany) maintained at 37 °C. Sink conditions for AmpB were maintained in each tube. At predetermined time intervals (15 min, 1, 2, 3, 4 and 5 hour), one tube was removed and the nanoparticles were precipitated using 1000 µl acetonitrile, followed by

centrifugation at 20 000 rpm for 10 minutes at 4 °C to pellet the particles. The amount of AmpB released was determined by analyzing the supernatant using the HPLC system described above after correction for free AmpB. Three independent runs were conducted and the results are expressed as mean \pm standard deviation.

Since the formulations were designed for absorption from the upper gastrointestinal tract, the effect of variable pH on the retention of AmpB within the AmpB NLC and ChiAmpB NLC formulations were investigated. A 1:20 v/v dilution of the formulations in phosphate buffer pH 5.8 (British Pharmacopeia) representing the proximal small intestine were firstly incubated for 2 hours, followed by adjustment of the pH to 6.8 (distal small intestine) with 6 μ l of 3M NaOH and further incubated for 4 hours (Ovesen et al. 1986; Evans et al. 1988). The percentage of AmpB retained in the formulations were determined similarly as described above.

2.6. Mucoadhesion studies

The mucoadhesive properties of the AmpB NLC and ChiAmpB NLC formulations were determined turbidimetrically after dispersing the formulations in type III porcine gastric mucin (Bonferoni et al. 2010; Sandri et al. 2017). The mucin was dispersed in buffered pH solutions (pH 5.8 and 6.8) under mild stirring at 0.05, 0.1, 0.25, 0.5, 0.75, 1.0 % w/v concentrations prior to admixture with the formulations at 1:1 v/v ratio. The mixture was incubated at 37 °C for and rotated on a shaker (WiseCube®, Witeg Inc., Germany) at 120 rpm for 2 hours. The absorbance of each mixture was measured using a UV-visible spectrophotometer (Epoch Microplate Spectrophotometer, Bio Tek Instruments, USA) at 650 nm. Pure chitosan was admixed with mucin as a control. Measurements were performed in triplicate and results were expressed as mean \pm standard deviation. A measure of the interaction between the formulations and mucin was determined as the difference in absorbance (ΔA) between the measured absorbance of formulation-mucin mixture (A) and theoretical absorbance (A_{theor}). The A_{theor} was determined as the sum of the absorbances from respective formulations with that of mucin solutions. The inference on mucoadhesion was based on the algorithm $\Delta A = 0$ means no interactions took place whilst $\Delta A \geq 0$ means strong interaction between mucin and the formulations (Bonferoni et al. 2010; Sandri et al. 2017).

2.7. Stability studies

The AmpB NLC and ChiAmpB NLC formulations were stored at 4 °C and protected from light. Aliquots were withdrawn at appropriate time intervals and the particle size, PDI, ζ and aggregation state were evaluated.

The effect of variation in pH on the physical properties of AmpB NLC and ChiAmpB NLC formulations was also studied by means of changes in the particle size and ζ . 50 μ l of the formulations were mixed in 950 μ l of phosphate buffer, pH 5.8 and 6.8 (British Pharmacopeia). The samples were incubated at 37 °C using a rotary shaker operated at 120 rpm for 2 hours. The changes in the particle size and ζ were evaluated using Zetasizer Nano ZS (Malvern, UK).

2.8. Statistical analyses

Statistical evaluation was performed using one-way analysis of variance (ANOVA), Tukey's post hoc test was conducted for multiple comparison between groups and differences were considered significant when $p < 0.05$. All calculations were conducted using IBM SPSS Statistics 24 (IBM cooperation, New York, NY).

3. Results and discussion

Since AmpB is poorly soluble in aqueous media, incorporation of AmpB during formulation without organic aids poses a challenge. In this work, we exploit the alkaline pH solubility profile of AmpB in incorporating AmpB into the NLC formulations (Santos et al. 2012; Caldeira et al. 2015). AmpB is soluble in aqueous media but only at extreme pH values ($\text{pH} < 2$ and > 11) whereby, the alkaline condition presents the safer monomer conformation of AmpB (Gagoś et al. 2008).

The AmpB NLC and ChiAmpB NLC were optimized (data not shown) prior to the commencement of the present study. The effect of mode of AmpB incorporation during the formulation of the AmpB NLC and ChiAmpB NLC was assessed based on particle size, polydispersity index (PDI) and zeta potential (ζ), and presented in Table 1.

10 mg of AmpB was added during formulation of the NLC either in undissolved state (UAmPB)

Method		Particle size (nm)		PDI		Zeta potential (mV)	
		AmpB NLC	ChiAmpB NLC	AmpB NLC	ChiAmpB NLC	AmpB NLC	ChiAmpB NLC
1	UAmPB	180.6±2.4	265.5±2.3	0.21±0.01	0.34±0.05	-44.8±0.4	27.4±0.5
	DAmPB	199.6±4.4	1141±28	0.28±0.01	0.22±0.03	-63.3±0.8*	17.5±1.4
2	DAmPB	140.5±1.0	175.5±1.2	0.11±0.02	0.20±0.03	-51.5±0.7*	-31.7±0.2

Table 1: Particle size, PDI and zeta potential values of NLCs as a function of mode of AmpB (10 mg) incorporation

or dissolved in 0.1 M NaOH (DAmpB) (section 2.2). The formed NLC formulations were then coated with chitosan. Regardless of the stage of AmpB incorporation, the particle size of the NLC formulations were below 200 nm, which is desirable in the present pursuit. Furthermore, the PDI values were all below 0.3 indicating that the formulations are homogeneous (Tan & Billa 2014). The ζ were strongly negative, ranging from -44 to -63 mV, which is indicative of high repulsive threshold against van der Waals interactions (Neupane et al. 2014). Aptly, the ζ of NLC obtained at both steps of addition of DAmpB were significantly higher than those from UAmPB ($p < 0.005$), indicating that more anionic components were adsorbed within the Helmholtz layer of the UAmPB NLC nanoparticles (Tan et al. 2010; Kumar et al. 2010). The adsorption of chitosan onto the NLC formulations was confirmed in all the cases by a significant increase in particle size ($p < 0.005$). Furthermore, since chitosan is positively charged under the formulation conditions, the changes in ζ values were all towards positivity, reaffirming the physical adsorption of chitosan onto the NLC nanoparticles (Ying et al. 2011; Ridolfi et al. 2012). In method 1, there was an increase in size of the ChiAmpB NLC formulated using UAmPB by about 84 nm. There was also an increase in size of the ChiAmpB NLC formulated with DAmpB by almost five-fold (1141 ± 28 nm) using method 1 and an increase of 35 nm using method 2. Further characterisation on the DAmpB NLC using method 1 was not carried out because of the significant increase in size of the NLC after the coating which is not

practically applicable in the present pursuit. Furthermore, physical instability during storage would have to be contended with. An increase in AmpB cargo within the NLC was carried out on UAmPB (method 1) and DAmPB (method 2) at a 50 mg AmpB threshold and a stability study was carried out on the resulting formulations. The results on particle size, PDI and ζ of the AmpB NLC and the chitosan-coated counterpart (ChiAmpB NLC) from both methods are presented in Table 2.

	Day	Particle size (nm)		PDI		Zeta potential (mV)	
		AmpB	ChiAmpB	AmpB	ChiAmpB	AmpB	ChiAmpB
		NLC	NLC	NLC	NLC	NLC	NLC
Method 1 <i>(UAmPB)</i>	1	163.1±0.7	348.0±12	0.19±0.01	0.42±0.09	-42.4±1.2	24.3±1.4
	35	160.6±1.8	331.4±3.6	0.16±0.03	0.47±0.02	-39.2±0.5*	21.8±0.3
	120	161.0±1.4	284.8±7.3*	0.19±0.03	0.38±0.07	-38.4±0.9*	20.0±1.8*
Method 2 <i>(DAmpB)</i>	1	142.6±0.1	184.7±1.6	0.11±0.02	0.26±0.03	-56.2±0.8	-31.4±0.6
	35	142.0±0.8	192.1±3.8*	0.12±0.02	0.26±0.04	-54.4±0.8	-30.5±1.4
	120	140.2±2.3	198.3±2.1*	0.15±0.01	0.26±0.01	-57.2±0.6	-32.2±2.5

Table 2: Effect of storage on physical properties of NLC at 50 mg cargo load of AmpB

There was a slight decrease in particle sizes of the uncoated NLC series (AmpB NLC) formulated using method 1 with 50 mg UAmPB compared to the previous uncoated series formulated with 10 mg of UAmPB (Table 1). However as in the initial series (Table 1), there was a decrease in size of the NLC formulated using method 2 (DAmpB) compared to the method 1 (UAmPB). Interestingly, the size of the DAmpB NLC remained essentially unchanged after we increased the AmpB load from 10 to 50 mg. Furthermore, the particle size of the DAmpB NLC at 50mg AmpB load also remained essentially unchanged during storage from both methods over the 120-day study period: method 1 ($p = 0.102$) and method 2 ($p = 0.428$). On the other hand, after coating with chitosan there was an increase in the sizes of the ChiAmpB NLC at 50 mg AmpB load in both methods of NLC formulation. Furthermore, there was a significant increase in size of the ChiAmpB NLC formulated via method 2 as a function of storage time ($p = 0.039$), indicating that the formulations from this method may be

unstable upon long-term storage (Tan & Billa 2014). It is worth noting that there was a progressive reduction in the particle size and ζ of the ChiAmpB NLC formulated via method 1, from day 1 to 120. This can be explained by the fact that in order to lower the surface free energy of the system, the particles tend to minimize their surface area to volume ratio and thus, form larger particles at the expense of smaller ones. However, we inferred that in the case of the ChiAmpB NLC system, the chitosan imparted stability via slow rearrangement of the polymer chains at the interface during storage so that the layer became tightened around the NLC. This ultimately resulted in the formation of smaller particles over time (Tan et al. 2010; Kumar et al. 2010).

Figure 1 presents the UV absorbance spectra of AmpB (UAmpB) within the NLC formulations from both methods at 10mg AmpB. Depending on the external milieu, AmpB may conform to either the monomer, dimer or polyaggregate state which can be detected readily by UV-visible spectroscopy (Barwicz et al. 1992). AmpB dissolved in 0.1 M NaOH (pH = 13) exhibits absorption spectra traditionally assigned to the monomer conformation with five distinctive absorption bands (407, 384, 365, 348 and 333 nm) with the highest intensity over the long-wavelength region (Gagoś et al. 2008).

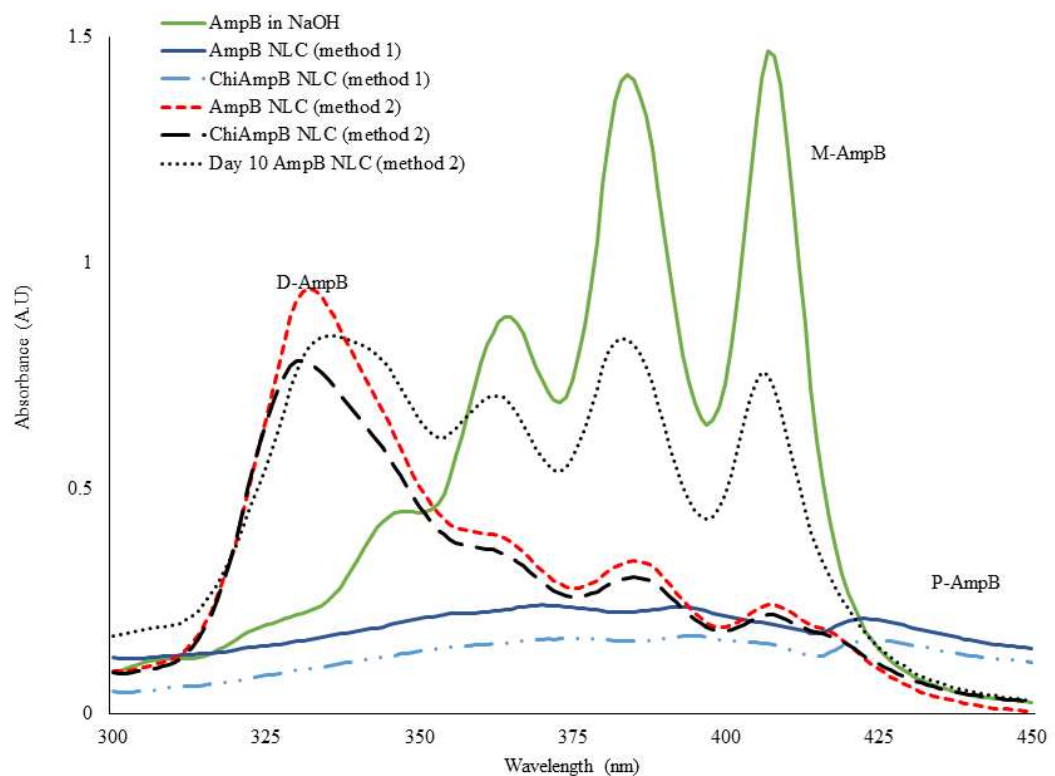


Figure 1: Absorption spectra corresponding to AmpB and ChiAmpB NLC formulations from method 1& 2. [M = monomer conformation, D = dimer and P = polyaggregate conformation of AmpB]

These distinctive peaks are absent in the absorption spectra displayed by AmpB in the NLC formulation prepared using method 1, where the spectra has been assigned to the polyaggregate form of AmpB (Espada et al. 2008). AmpB NLC prepared via method 2 displays only four of the five distinct absorption peaks but with varied intensities (407, 385, 363 and 332 nm). The principal absorption peak occurs at 332 nm indicating that the dimer conformation is the predominant form in this NLC formulation (Bianco et al. 2010). However, after 10 days of storage, the absorbance intensity at the short-wavelength region dropped by 11 % with a red-shift in wavelength towards 335 nm while the absorbance at 407 nm, increased by 3-fold. This suggests a growth in the aggregation state of AmpB in NLC prepared by method 2 to the monomer conformation during storage. The absorption spectra for ChiAmpB NLC prepared via method 1 presented a similar pattern as the

uncoated NLC formulation but with lower absorbance intensities. Likewise, the absorption spectra from ChiAmpB NLC prepared by method 2 mirrors the spectra of the uncoated NLC which is attributable to the dimer conformation.

The aggregation ratio within each formulation was obtained as the ratio of the absorbance at 332 nm (peak of the dimer) to that at 407 nm (peak of the monomer). An aggregation ratio > 1 indicates that more than 50 % of the AmpB is in the aggregated state while ratio < 0.2 reflects nearly 100 % monomer form. The aggregation ratios of AmpB in uncoated and chitosan coated NLC prepared by method 1 were all below 1 over a 120-day period, indicating a predominantly monomeric conformation (Figure 2).

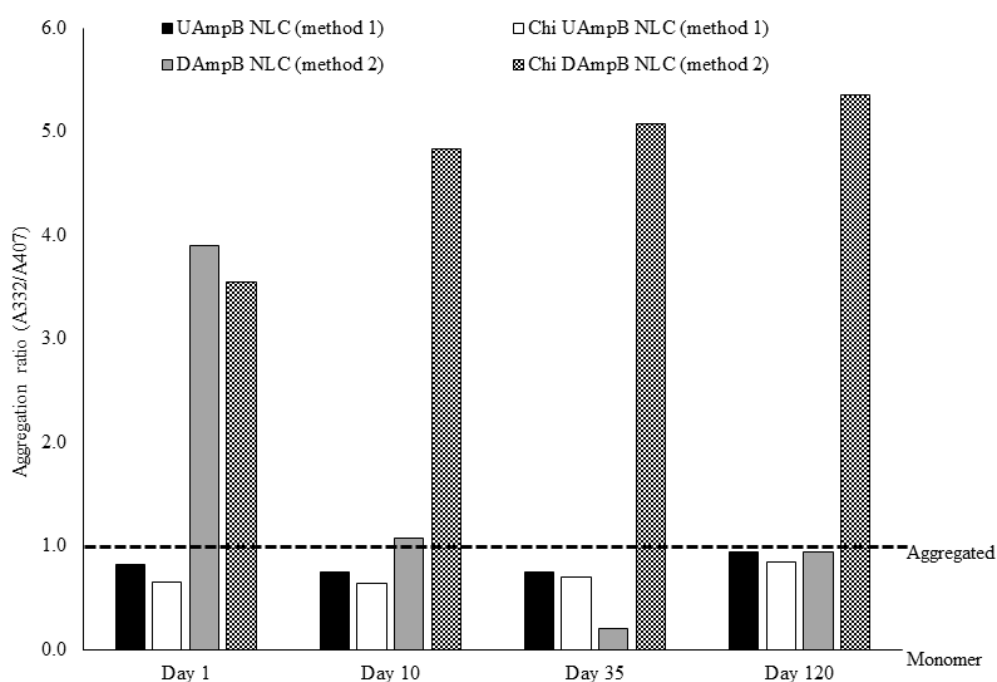


Figure 2: Extent of AmpB aggregation in NLC and ChiNLC formulations over 120-day study period

Thus, we inferred that AmpB in uncoated and chitosan-coated NLC prepared by method 1 is a mixture of polyaggregates (Figure 1) and monomers (Figure 2), with latter being dominant. Both

polyaggregate and monomer are known to be less toxic than the dimer conformation in *in vitro* mammalian cells and *in vivo* mice studies (Gaboriau et al. 1997; Bartlett et al. 2004; Espada et al. 2008). On the other hand, the extent of AmpB aggregation in the NLC formulation prepared by method 2 decreased over time from a highly aggregated state (3.9) that fell to 0.2 on day 35, which is indicative of growth of AmpB to the monomeric state during storage. There was a slight increase in the aggregation ratio on day 120 however this was still below the threshold 1. However, after coating with chitosan, AmpB (method 2) remained in the aggregated state throughout the 120-day study period. In fact, it appears that the aggregated state grew over time. Clearly, the mode of incorporation of AmpB is crucial in determining the ultimate conformation. Due to the dimer conformation of AmpB and the instability of the formulations from method 2, further studies were discontinued using this method and focus is now on AmpB NLC and ChiAmpB NLC formulations using method 1.

Figure 3 shows the STEM images of the AmpB NLC and ChiAmpB NLC formulations whereby the nanoparticles appeared to be spherical and discrete. The particle sizes from both AmpB NLC and ChiAmpB NLC formulations are in agreement with the results obtained in Table 2. The average encapsulation efficiency of AmpB NLC formulation was 83.4 ± 0.72 % with drug loading of 12.3 ± 0.11 % (Table 3). This high % EE and % DL can be attributed to the high lipophilicity of

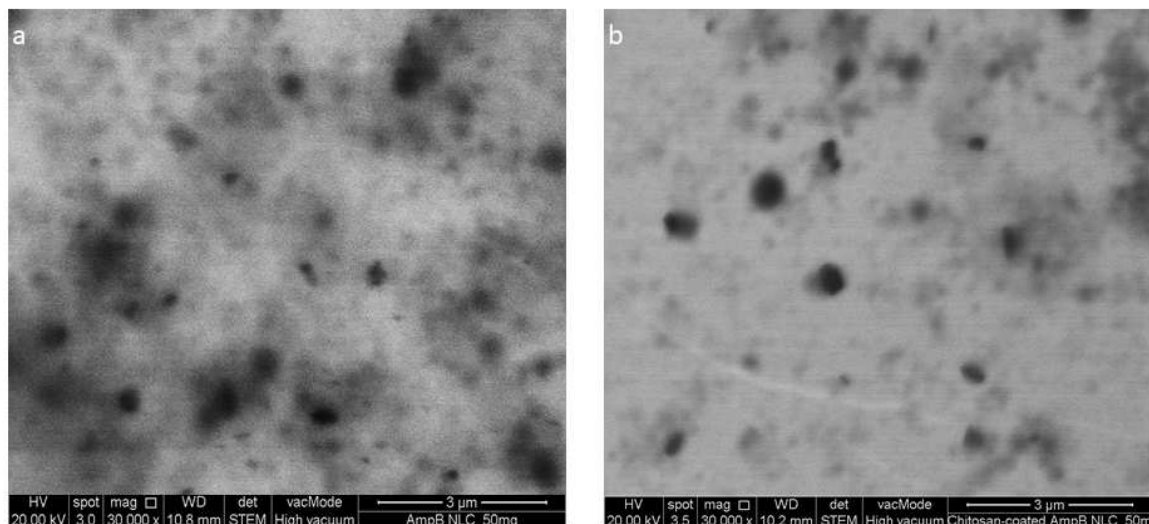


Figure 3: STEM image of (a) AmpB NLC and (b) ChiAmpB NLC formulations

AmpB and the imperfect crystal of the NLC system provided by the coconut oil (Ridolfi et al. 2012; Lv et al. 2016). Upon addition of chitosan coating, the mean encapsulation efficiency showed a significant increase of about 3% ($p < 0.0005$) which is in accordance with another study (Li et al. 2016).

	AmpB NLC	ChiAmpB NLC
Encapsulation efficiency (%)	83.4 ± 0.72	$86.0 \pm 0.33^*$
Drug loading (%)	12.3 ± 0.11	11.0 ± 0.04

Table 3. Encapsulation efficiency and drug loading of AmpB NLC and ChiAmpB NLC formulations.

This suggests that there is an interaction between the cationic moiety of chitosan polymer coating with the anionic segment of the NLC nanoparticles which prevents the expulsion of the AmpB (Li et al. 2016). This assertion is supported by an earlier observation that the ChiAmpB NLC prepared

by method 1 decreased in size during storage. We attributed this to the reorganisation of the chitosan polymer chains on the surface of the NLC in manner that tightens the structure that ensures the AmpB is retained.

The release studies of AmpB from the NLC was carried out on AmpB NLC and ChiAmpB NLC formulations prepared using method 1. The release medium was phosphate buffer pH 7.4 containing 1% Tween - 80. Free AmpB (control) showed rapid release, $97.6 \pm 0.1\%$ of AmpB being released within 15 minutes and this is in accordance with study by Jain et al. 2014. In contrast, both formulations showed a biphasic release profile, with a burst release observed initially, followed by a more sustained release, as presented in Figure 4a (Hu et al. 2005).

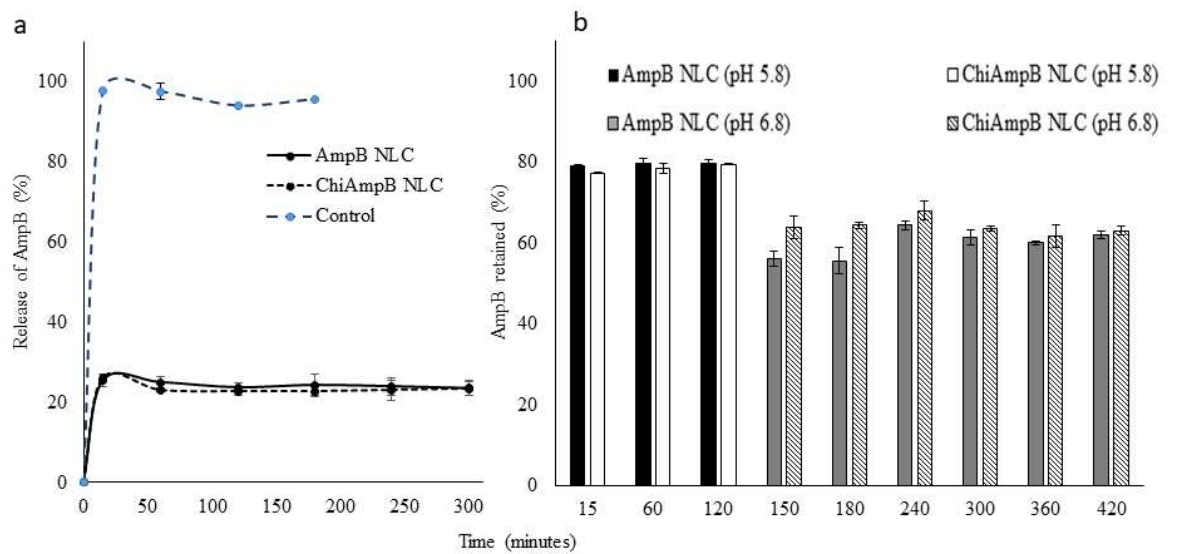


Figure 4: (a) Percentage release of pure Amp B (control) compared with AmpB from NLC and ChiNLC formulations in pH 7.4 containing 1% Tween-80 and (b) percentage retention of AmpB in pH 5.8 & 6.8 media

The burst release during the first 15 minutes suggests the presence of some of the coconut oil at the surface of the NLC due to a difference in the melting points of the beeswax and coconut oil so that the former begins to crystallise before the latter during the cooling process of the NLC. The crystallisation extrudes some of the coconut oil to the surface as it carries part of the dissolved AmpB along. Therefore there is a regional accumulation of AmpB at the outer region of NLC which is released as in a burst (Hu et al. 2005; Teeranachaideekul et al. 2007). Furthermore, the release profiles of AmpB from AmpB NLC and ChiAmpB NLC formulation were superimposable, albeit a slightly lower release from the ChiAmpB NLC which can be attributed to impedance in diffusion of AmpB by the chitosan barrier coating.

The extent to which AmpB was retained within the formulations after dispersion in media at pH 5.8 and 6.8 media is presented in Figure 4b. pH 5.8 is the typical pH of the proximal small intestine whilst pH 6.8 represents the distal small intestine. Only about 20 % of AmpB was expelled from both AmpB NLC and ChiAmpB NLC formulations during incubation in pH 5.8 in the first two hours ($p = 0.484$). In order to mimic the gastrointestinal transit from duodenum, jejunum to ileum, the pH of the medium was raised to 6.8, by the addition of 6 μ l of 3M NaOH. After only 30 minutes of incubation in media with pH 6.8, the percentage of AmpB retained in the AmpB NLC and ChiAmpB NLC formulations were $56.1 \pm 1.8 \%$ and $63.9 \pm 2.8 \%$ respectively. Thus it apparent that the chitosan coating shielded AmpB from expulsion from the NLC (Yang et al. 2012).

In a parallel study, the effect of variable pH on changes in the physical properties of the formulations in terms of particle size and ζ were conducted and presented in Figure 5.

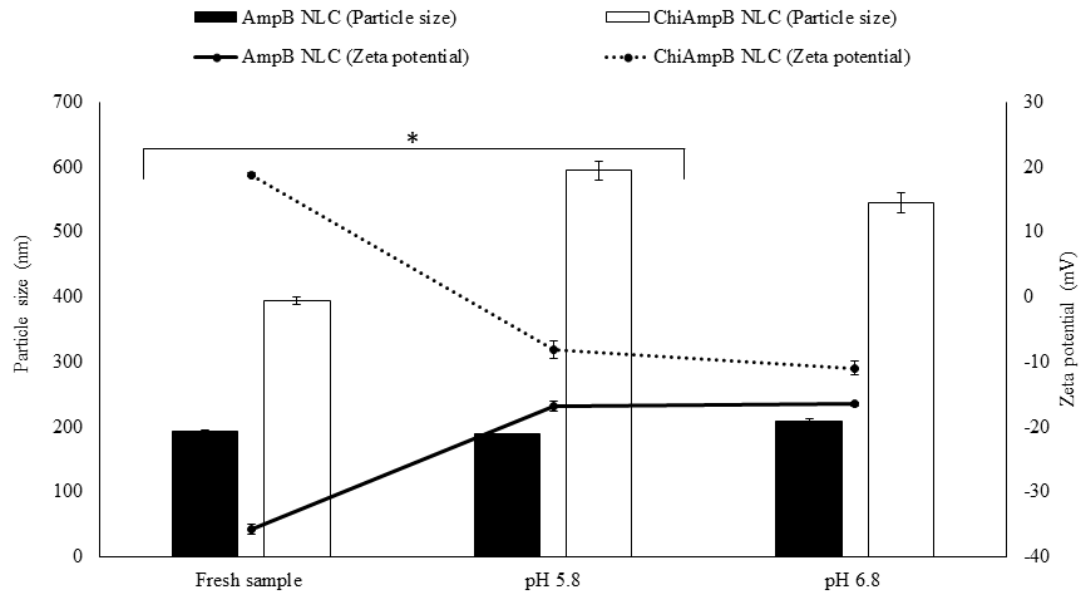


Figure 5: Stability of AmpB NLC and ChiAmpB NLC formulations after exposure to pH 5.8 and 6.8

There was no significant change in the particle size of the AmpB NLC formulation in pH 5.8 medium ($p = 0.332$). Although there was a slight increase in particle size in pH 6.8 ($p=0.003$), it was not aggregation-related since the final particle size remained at 208.1 ± 5.0 nm. Despite a decrease in ζ values of AmpB NLC formulation of approximately 19 mV, to -16.9 ± 0.8 (pH 5.8) and -16.5 ± 0.3 mV (pH 6.8), the formulation remained essentially stable as reflected via the particle sizes, which suggests that adequate electrostatic repulsion was maintained among the particles, that prevented agglomeration (Amekyeh et al. 2017). In pH 5.8 and 6.8 media, the ChiAmpB NLC formulation registered a two-fold increase in particle size with a marked drop in ζ , from $+18.8 \pm 0.3$ to -8.1 ± 1.4 (pH 5.8) and -10.9 ± 1.1 mV (pH 6.8). This suggests the neutralisation of the positive charge density

on fresh ChiAmpB NLC by the anions present in the phosphate buffer. The reduction in the ζ favour the van der Waals interactions which result in the increase in particle size of the nanoparticles (Bhattacharjee 2016).

The mucoadhesive properties of two types of NLC formulations were evaluated based on turbidimetric measurements which measures the increase in turbidity of the system as particles agglomerate resulting from the adsorption of mucin onto the nanoparticles (Bonferoni et al. 2010; Yostawonkul et al. 2017). Figure 6 (a and b) illustrates the change in absorbance values (ΔA) as a function of mucin concentrations at pH 5.8 and 6.8 respectively. In both pH conditions, AmpB NLC formulation presented positive change in absorbance values albeit negatively charged.

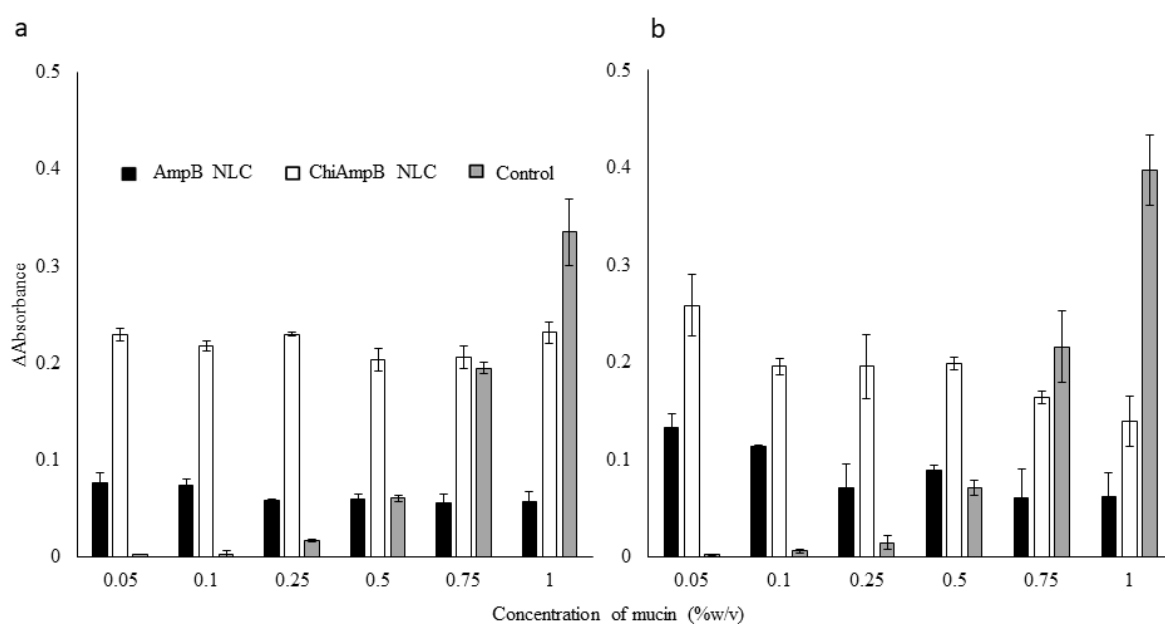


Figure 6: Turbidimetric measurements in (a) pH 5.8 and (b) 6.8 media

This suggests that possible interaction between the formulation and the cations present in the phosphate buffer, presumably provided by potassium ions (Luo et al. 2015; Sandri et al. 2017).

Crucially, the ChiAmpB NLC formulation presented a significantly larger positive change in absorbance values compared to AmpB NLC formulation in both pH conditions. We may conclude that mucoadhesion properties of the ChiAmpB NLC formulation is mostly driven by electrostatic interactions between positively charged chitosan and negatively charged (COO⁻) mucin protein (He et al. 1998; Rençber et al. 2016).

4. Conclusions

An AmpB-containing NLC was successfully formulated which demonstrated mucoadhesive properties at pH values representing possible absorption regions in the small intestine. Based on a previous study, we believe this formulation has the potential for improved uptake from the small intestine due to mucoadhesion and hence improved bioavailability of AmpB. Furthermore, the UAmpB-containing NLC formulations is more stable and presented the safer conformation of AmpB compared to DAmpB-containing NLC formulation. Therefore, this formulation is primed for studies to affirm the improved pharmacokinetics of AmpB whilst at the same time the toxicity concerns have been addressed.

Declaration

The authors have no declaration to report

References

- Amekyeh, H., Billa, N., Yuen, K. & Chin, L.S., 2015. A gastrointestinal transit study on amphotericin B-loaded solid lipid nanoparticles in rats. *AAPS PharmSciTech*, 16(12), pp.871–877.
- Amekyeh, H., Billa, N. & Roberts, C., 2017. Correlating gastric emptying of amphotericin B and paracetamol solid lipid nanoparticles with changes in particle surface chemistry. *International Journal of Pharmaceutics*, 517(1-2), pp.42–49.
- Bartlett, K., Yau, E., Hartsel, S.C., Hamer, A., Tsai, G., Bizzotto, D., Wasan, K.M., 2004. Effect of heat-treated amphotericin B on renal and fungal cytotoxicity. *Antimicrobial Agents and Chemotherapy*, 48(1), pp.333–336.
- Barwicz, J., Christian, S. & Gruda, I., 1992. Effects of the aggregation state of amphotericin B on its toxicity to mice. *Antimicrobial Agents and Chemotherapy*, 36(10), pp.2310–2315.

420 Benincasa, M., Pacor, S., Wu, W., Prato, M., Bianco, A., Gennaro, R., 2011. Antifungal activity of
421 amphotericin B conjugated to carbon nanotubes. *ACS Nano*, 5(1), pp. 199-208.

422 Bhattacharjee, S., 2016. DLS and zeta potential – what they are and what they are not? *Journal of*
423 *Controlled Release*, 235, pp.337–351.

424 Bianco, M.A., Gallarate, M., Trotta, M. & Battaglia, L., 2010. Amphotericin B loaded SLN prepared
425 with the coacervation technique. *Journal of Drug Delivery Science and Technology*, 20(3), pp.187–
426 191.

427 Bonferoni, M.C., Sandri, G., Ferrari, F., Rossi, S., Larghi, V., Zambito, Y. & Caramella, C., 2010.
428 Comparison of different *in vitro* and *ex vivo* methods to evaluate mucoadhesion of glycol-palmitoyl
429 chitosan micelles. *Journal of Drug Delivery Science and Technology*, 20(6), pp.419–424.

430 Butani, D., Yewale, C. & Misra, A., 2016. Topical amphotericin B solid lipid nanoparticles: design
431 and development. *Colloids and Surfaces B: Biointerfaces*, 139, pp.17–24.

432 Caldeira, L.R., Fernandes, F.R., Costa, D.F., Frezard, F., Afonso, L.C.C. & Ferreira, L.A.M., 2015.
433 Nanoemulsions loaded with amphotericin B: a new approach for the treatment of leishmaniasis.
434 *European Journal of Pharmaceutical Sciences*, 70, pp.125–131.

435 Chaudhari, M.B., Desai, P.P., Patel, P.A., 2016. Solid lipid nanoparticles of amphotericin B
436 (AmbiOnp): *in vitro* and *in vivo* assessment towards safe and effective oral treatment module. *Drug*
437 *Delivery and Translational Research*, 6, pp. 354-364.

438 Espada, R., Valdespina, S., Dea, M.A., Molero, G., Ballesteros, M.P., Bolas, F. & Torrado, J.J., 2008.
439 Effect of aggregation state on the toxicity of different amphotericin B preparations. *International*
440 *Journal of Pharmaceutics*, 361(1-2), pp.64–69.

441 Evans, D.F., Pye, G., Bramley, R., Clark, A.G., Dyson, T.J., Hardcastle, J.D., 1988. Measurement of
442 gastrointestinal pH profiles in normal ambulant human subjects. *Gut*, 29(8), pp.1035–1041.

443 Gagoś, M., Koper, R. & Gruszecki, W.I., 2008. Anomalously high aggregation level of the polyene
444 antibiotic amphotericin B in acidic medium: implications for the biological action. *Biophysical*
445 *Chemistry*, 136(1), pp.44–49.

446 He, P., Davis, S.S. & Illum, L., 1998. *In vitro* evaluation of the mucoadhesive properties of chitosan
447 microspheres. *International Journal of Pharmaceutics*, 166(1), pp.75–88.

448 Hu, F.Q., Jiang, S., Du, Y., Yuan, H., Ye, Y. & Zeng, S., 2005. Preparation and characterization of
449 stearic acid nanostructured lipid carriers by solvent diffusion method in an aqueous system. *Colloids*
450 *and Surfaces B: Biointerfaces*, 45(3-4), pp.167–173.

451 Hussain, A., Singh, V.K., Singh, O.P., Shafaat, K., Kumar, S., Ahmad, F.J., 2016. Formulation and
452 optimization of nanoemulsion using antifungal lipid and surfactant for accentuated topical delivery of
453 amphotericin B. *Drug Delivery*, 23(8), pp. 3101-3110.

454 Italia, J.L., Yahya, M.M., Singh, D., Kumar, M.N.V.R., 2009. Biodegradable nanoparticles improve
455 oral bioavailability of amphotericin B and show reduced nephrotoxicity compared to intravenous
456 Fungizone®. *Pharmaceutical Research*, 26(6), pp. 1324-1331.

457 Jain, S., Valvi, P.U., Swarnakar, N.K., Thanki, K., 2012. Gelatin coated hybrid lipid nanoparticles for
458 oral delivery of amphotericin B. *Molecular Pharmaceutics*, 9(9), pp. 2542-2553.

459 Jain, V., Gupta, A., Pawar, V.K., Asthana, S., Jaiswal, A.K., Dube, A., Chourasia, M.K., 2014.
460 Chitosan-assisted immunotherapy for intervention of experimental leishmaniasis via amphotericin B-
461 loaded solid lipid nanoparticles. *Application Biochemistry Biotechnology*, 174, pp. 1309-1330.

462 Jung, S.H., Lim, D.W., Jung, S.H., Lee, J.E., Jeong, K., Seong, H. & Shin, B.C., 2009. Amphotericin
463 B-entrapping lipid nanoparticles and their *in vitro* and *in vivo* characteristics. *European Journal of*
464 *Pharmaceutical Sciences*, 37(3-4), pp.313–320.

465 Kayser, O., Olbrich, C., Yardley, V., Kiderlen, A.F. & Croft, S.L., 2003. Formulation of amphotericin
466 B as nanosuspension for oral administration. *International Journal of Pharmaceutics*, 254(1), pp.73–
467 75.

468 Kumar, V., Adamson, D.H. & Prud'homme, R.K., 2010. Fluorescent polymeric nanoparticles:
469 aggregation and phase behavior of pyrene and amphotericin B molecules in nanoparticle cores. *Small*,
470 6(24), pp.2907–2914.

471 Lance, M.R., Washington, C. & Davis, S.S., 1995. Structure and toxicity of amphotericin B /
472 triglyceride emulsion formulations. *Journal of Antimicrobial Chemotherapy*, 36, pp.119–128.

473 Legrand, P., Romero, E.A., Cohen, B.E. & Bolard, J., 1992. Effects of aggregation and solvent on the
474 toxicity of amphotericin B to human erythrocytes. *Antimicrobial Agents and Chemotherapy*, 36(11),
475 pp.2518–2522.

476 Li, J., Liu, D., Tan, G., Zhao, Z., Yang, X. & Pan, W., 2016. A comparative study on the efficiency of
477 chitosan-N-acetylcysteine, chitosan oligosaccharides or carboxymethyl chitosan surface modified
478 nanostructured lipid carrier for ophthalmic delivery of curcumin. *Carbohydrate Polymers*, 146,
479 pp.435–444.

480 Liu, M., Chen, M. & Yang, Z., 2017. Design of amphotericin B oral formulation for antifungal
481 therapy. *Drug Delivery*, 24(1), pp.1–9.

482 Luo, Y., Teng, Z., Li, Y. & Wang, Q., 2015. Solid lipid nanoparticles for oral drug delivery: chitosan
483 coating improves stability, controlled delivery, mucoadhesion and cellular uptake. *Carbohydrate*
484 *Polymers*, 122, pp.221–229.

485 Lv, W., Zhao, S., Yu, H., Li, N., Garamus, V.M., Chen, Y., Yin, P., Zhang, R., Gong, Y. & Zou, A.,
486 2016. Brucea javanica oil-loaded nanostructure lipid carriers (BJO NLCs): preparation,
487 characterization and *in vitro* evaluation. *Colloids and Surfaces A: Physicochem. Eng. Aspects*, 504,
488 pp.312–319.

489 Muchow, M., Maincent, P. & Muller, R.H., 2008. Lipid nanoparticles with a solid matrix (SLN, NLC,
490 LDC) for oral drug delivery. *Drug development and industrial pharmacy*, 34(12), pp.1394–405.

491 Nahar, M., Mishra, D., Dubey, V., Jain, N.K., 2008. Development, characterization, and toxicity
492 evaluation of amphotericin B-loaded gelatin nanoparticles. *Nanomedicine: Nanotechnology, Biology,*
493 *and Medicine*, 4, pp. 252-261.

494 Neupane, Y.R., Srivastava, M., Ahmad, N., Kumar, N., Bhatnagar, A. & Kohli, K., 2014. Lipid based
495 nanocarrier system for the potential oral delivery of decitabine: Formulation design, characterization,
496 *ex vivo*, and *in vivo* assessment. *International Journal of Pharmaceutics*, 477(1-2), pp.601–612.

497 Ovesen, L., Bendtsen, F., Tage-Jensen, U., Pedersen, N.T., Gram, B.R., Rune, S.J., 1986. Intraluminal
498 pH in the stomach, duodenum, and proximal jejunum in normal subjects and patients with exocrine
499 pancreatic insufficiency. *Gastroenterology*, 90(4), pp.958–962.

500 Radwan, M.A., AlQuadeib, B.T., Siller, L., Wright, M.C. & Horrocks, B., 2017. Oral administration
501 of amphotericin B nanoparticles: antifungal activity, bioavailability and toxicity in rats. *Drug*
502 *Delivery*, 24(1), pp.40–50.

503 Rençber, S., Karavana, S.Y., Yilmaz, F.F., Erac, B., Nenni, M., Ozbal, S., Pekcetin, C., Gurer-Orhan,
 504 H., Hosgor-Limoncu, M., Guneri, P. & Ertan, G., 2016. Development, characterization, and *in vivo*
 505 assessment of mucoadhesive nanoparticles containing fluconazole for the local treatment of oral
 506 candidiasis. *International Journal of Nanomedicine*, 11, pp.2641–2653.

507 Ridolfi, D.M., Marcato, P.D., Justo, G.Z., Cordi, L., Machado, D. & Duran, N., 2012. Chitosan-solid
 508 lipid nanoparticles as carriers for topical delivery of tretinoin. *Colloids and Surfaces B: Biointerfaces*,
 509 93, pp.36–40.

510 Sandri, G., Motta, S., Bonferoni, M.C., Brocca, P., Rossi, S., Ferrari, F., Rondelli, V., Cantu, L.,
 511 Caramella, C. & Favero, E.D., 2017. Chitosan-coupled solid lipid nanoparticles: tuning nanostructure
 512 and mucoadhesion. *European Journal of Pharmaceutics and Biopharmaceutics*, 110, pp.13–18.

513 Santangelo, R., Paderu, P., Delmas, G., Chen, Z., Mannino, R., Zarif, L., Perlin, D.S., 2000. Efficacy
 514 of oral cochleate-amphotericin B in a mouse model of systemic candidiasis. *Antimicrobial Agents and*
 515 *Chemotherapy*, 44, pp. 2356-2360.

516 Santos, C.M., Oliveira, R.B., Arantes, V.T., Caldeira, L.R., Oliveira, M.C., Egito, E.S.T. & Ferreira,
 517 L.A.M., 2012. Amphotericin B-loaded nanocarriers for topical treatment of cutaneous leishmaniasis:
 518 Development, characterization, and *in vitro* skin permeation studies. *Journal of Biomedical*
 519 *Nanotechnology*, 8(2), pp.322–329.

520 Silva, A.E., Barratt, G., Cheron, M. & Egito, E.S.T., 2013. Development of oil-in-water
 521 microemulsions for the oral delivery of amphotericin B. *International Journal of Pharmaceutics*,
 522 454(2), pp.641–648.

523 Tan, S.W., Billa, N., Roberts, C.R. & Burley, J.C., 2010. Surfactant effects on the physical
 524 characteristics of amphotericin B-containing nanostructured lipid carriers. *Colloids and Surfaces A:*
 525 *Physicochemical and Engineering Aspects*, 372(1-3), pp.73–79.

526 Tan, S.W. & Billa, N., 2014. Lipid effects on expulsion rate of amphotericin B from solid lipid
 527 nanoparticles. *AAPS PharmSciTech*, 15(2), pp.287–95.

528 Teeranachaideekul, V., Souto, E.B., Junyaprasert, V.B. & Muller, R.H., 2007. Cetyl palmitate-based
 529 NLC for topical delivery of Coenzyme Q10 - Development, physicochemical characterization and *in*
 530 *vitro* release studies. *European Journal of Pharmaceutics and Biopharmaceutics*, 67(1), pp.141–148.

531 Van de Ven, H., Paulussen, C., Feijens, P.B., Matheeussen, A., Rombaut, P., Kayaert, P., Van den
 532 Mooter, G., Weyenberg, W., Cos, P., Maes, L., Ludwig, A., 2012. PLGA nanoparticles and
 533 nanosuspensions with amphotericin B: potent *in vitro* and *in vivo* alternatives to Fungizone and
 534 AmBisome. *Journal of Controlled Release*, 161, pp. 795-803.

535 Wasan, E.K., Bartlett, K., Gershkovich, P., Sivak, O., Banno, B., Wong, Z., Gagnon, J., Gates, B.,
 536 Leon, C.G., Wasan, K.M., 2009. Development and characterization of oral lipid-based amphotericin B
 537 formulations with enhanced drug solubility, stability and antifungal activity in rats infected with
 538 *Aspergillus fumigatus* or *Candida albicans*. *International Journal of Pharmaceutics*, 372, pp. 76-84.

539 Yang, Z., Tan, Y., Chen, M., Dian, L., Shan, Z., Peng, X. & Wu, C., 2012. Development of
 540 amphotericin B-loaded cubosomes through the SolEmuls technology for enhancing the oral
 541 bioavailability. *AAPS PharmSciTech*, 13(4), pp.1483–91.

542 Ying, X.Y., Cui, D., Yu, L. & Du, Y.Z., 2011. Solid lipid nanoparticles modified with chitosan
 543 oligosaccharides for the controlled release of doxorubicin. *Carbohydrate Polymers*, 84(4), pp.1357–
 544 1364.

545 Yoon, G., Park, J.W. & Yoon, I., 2013. Solid lipid nanoparticles (SLNs) and nanostructured lipid
 546 carriers (NLCs): recent advances in drug delivery. *Journal of Pharmaceutical Investigation*, 43(5),
 547 pp.353–362.

548 Yostawonkul, J., Surassmo, S., Iempridee, T., Pimtong, W., Suktham, K., Sajomsang, W., Gonil, P. &
 549 Ruktanonchai, U.R., 2017. Surface modification of nanostructure lipid carrier (NLC) by oleoyl-
 550 quaternized-chitosan as a mucoadhesive nanocarrier. *Colloids and Surfaces B: Biointerfaces*, 149,
 551 pp.301–311.

552